DOI: 10.1002/anie.201309974

Surface Topography

Rapid Generation of Cell Gradients by Utilizing Solely Nanotopographic Interactions on a Bio-Inert Glass Surface**

*Gao Yang, Yanhua Cao, Junbing Fan, Hongliang Liu, Feilong Zhang, Pengchao Zhang, Chao Huang, Lei Jiang, and Shutao Wang**

Abstract: *The control of cell gradients is critical for understanding many biological systems and realizing the unique functionality of biomimetic implants. Herein, we report a nanotopographic gradient strategy that can rapidly generate cell gradients on a nanodendritic silica substrate without any chemical modification. We can achieve controllable cell gradients within only half an hour of cell incubation solely induced by the topographic effect of the gradient nanodendrites. We also demonstrate that cell gradients can be modulated by the combination of nanotopographic and chemical gradients. The results reveal that the enhanced topographic interactions between the nanodentritic structure and nanoscaled filopodia of the cells mainly contribute to the generation of cell gradients.*

Cell gradients are one of the most typical features of biological systems, and directly guide many biological processes, such as embryonic development[1] and the interface integration of tendon to bone.[2] Therefore, the ability to generate controllable cell gradients is important for understanding biological systems.[3] More importantly, cell gradients guide the design of biomimetic gradient implants,[4] such as dental gradient implants.[5] To date, several methodologies based on the variation of surface properties, such as surface chemistry,[6] stiffness of the substrate,[7] and surface electrical cue,[8] have been employed to generate cell gradients. Chemical gradient surfaces of adhesive molecules (e.g., fibronectin) are mostly used to establish local variations in cell density.[6a] Cell gradients have also been generated by directly guiding cell migration on stiffness gradient substrates.[7] Alternatively, Xia et al. developed an intelligent method to rapidly establish controllable cell gradients in only two hours by tilting a glass substrate into a cell suspension.[9] In general, in these approaches, surface modification with adhesive molecules is required to improve cell attachment and decrease the cell incubation time.

Glass-based biomaterials have long been recognized as promising biocompatible materials in applications such as cell culture plates[10] and implant materials.[11] However, the glass-based materials tend to suffer from other drawbacks particularly low cell affinity.[12] To render the inert surfaces bioactive, most existing technologies rely on chemical modification, such as collagen coating.[13] On the other hand, engineering the surface nanotopography has been recently proved as an effective strategy to modulate cell behavior, including adhesion, proliferation, migration, and differentiation.[14] For example, our group utilized nanostructured substrates, such as silicon nanopillars,[15] poly(3,4-ethylenedioxy)thiophene-COOH nanodots,[16] fractal gold nanostructures,[17] and nanodendritic silica,[18] to efficiently capture circulating tumor cells through enhanced topographic interactions. These results encouraged us to attempt to address the next challenge—the rapid generation of cell gradients by utilizing topographic interactions.

Herein, we demonstrate that a nanotopographic gradient strategy, solely by the introduction of gradient nanodendritic silica onto bio-inert glass surface, can rapidly establish cell gradients without any chemical modification (Figure 1a). Owing to the enhanced topographic interactions between gradient nanodendrites and nanoscaled filopodia on cell surface, we can rapidly achieve controllable cell gradients within only half an hour of cell incubation. In addition, we investigated the co-modulation of nanotopographic and chemical gradients on the cell gradient in such a short period.

In our experiment, we fabricated the nanodendritic gradient silica by combining the oblique deposition and the template coating methods[18,19] (Figure S1, and Section 2 in the Supporting Information). Firstly, we deposited a layer of carbon nanoparticles with a thickness gradient by placing the glass substrate on a carbon source at an oblique angle, θ (Figure S1a, Supporting Information). By simply changing the oblique angle, we can obtain a series of carbon nanoparticle layers with different gradients. Then, we coated the carbon nanoparticles with a silica shell by chemical vapor deposition of silicon tetrachloride,[20] and finally removed the template by calcination (Figure S1b, Supporting Information). This process yielded a series of nanodendritic silica gradients (Figure S2, Supporting Information). A typical nanotopographic gradient was characterized by scanning

[*] Dr. G. Yang, MSc. Y. Cao, Dr. J. Fan, Dr. H. Liu, Dr. F. Zhang, Dr. P. Zhang, Dr. C. Huang, Prof. L. Jiang, Prof. S. T. Wang
Beijing National Laboratory for Molecular Sciences (BNLMS)
Key Laboratory of Organic Solids Institute of Chemistry
Chinese Academy of Sciences
Beijing, 100190 (P.R. China)
E-mail: stwang@iccas.ac.cn
Dr. G. Yang, Dr. F. Zhang, Dr. P. Zhang
University of Chinese Academy of Sciences
Beijing 100049 (P.R. China)

[**] This research was supported by the National Research Fund for Fundamental Key Projects (2012CB933800, 2013CB933000, and 2012CB934100), the National Natural Science Foundation (21121001, 21127025, 21175140, and 20974113), the Key Research Program of the Chinese Academy of Sciences (KJZD-EW-M01), and the National High Technology Research and Development Program of China (863 Program) (2013AA031903).

Supporting information for this article is available on the WWW under http://dx.doi.org/10.1002/anie.201309974.

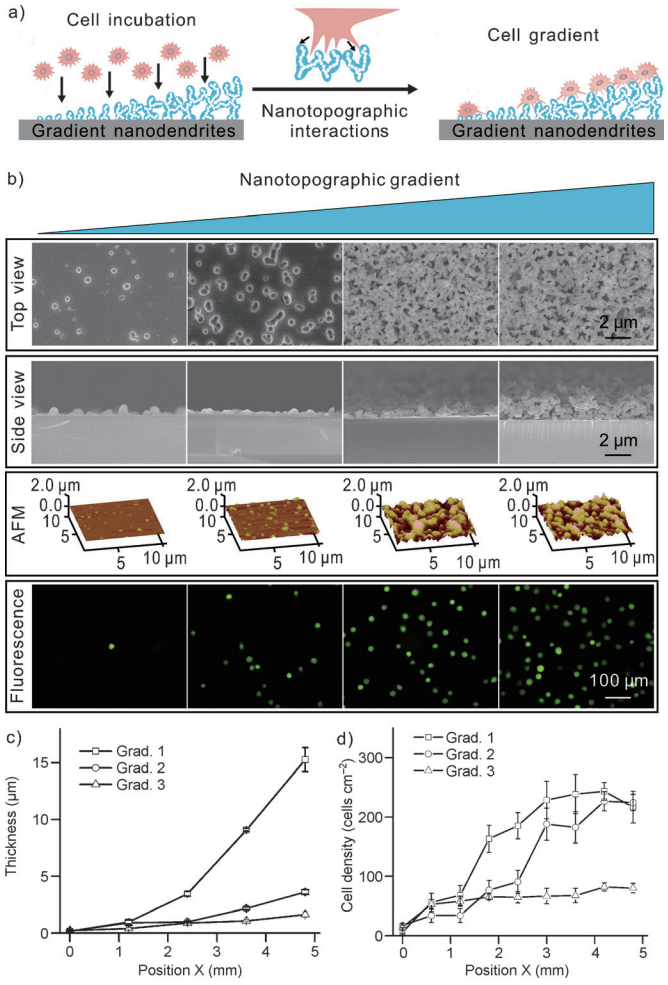

Figure 1. a) Schematic of the rapid generation of a cell gradient induced solely by a nanotopographic gradient within only half an hour after the substrate had been immersed into the cell suspension. b) On a typical nanotopographic gradient substrate (e.g. Grad. 2) a cell gradient was observed clearly. The nanotopographic gradient was characterized by top-view and side-view scanning electron microscope (SEM) and atom force microscope (AFM) images. The cells were prestained with Calcium AM (green) for visualization in fluorescence images. Magnifications are the same across individual rows. c,d) For the substrates with nanotopographic gradients, the thickness of the nanodendritic silica structure (c) and the cell density (d) were plotted against substrate position. With increasing values of θ in the deposition of the carbon nanoparticles from 0° to 15° to 30°, the nanotopographic gradient decreased, finally resulting in the minimal gradient in cell density. Error bars represent the standard error of mean from three measurements.

electron microscope (SEM) and atom force microscope (AFM) images (Figure 1b). The surface roughness, coverage, and thickness of the nanodendritic silica structure gradually increase along the surface of the nanotopographic gradient.

To demonstrate the capability of the nanotopographic gradient to induce cell gradients, we performed cell adhesion experiments on a representative nanodendritic gradient substrate. We first explored the influence of the incubation time between 5 and 90 min, on cell adhesion for the relatively uniform nanodendritic silica substrate and the flat glass substrate (Figures S3 and S4, Supporting Information). The greatest difference in cell numbers on the two substrates was observed at 30 min. Therefore, we immersed the nanodendritic gradient substrates in a suspension of NIH/3T3 cells (at a concentration of 2×10^5 cells mL^{-1}) and incubated for 30 min. Then, we rinsed the substrates and imaged the adhered cells. The number of adhered cells increased gradually along the surface with nanodendritic gradient, representing the rapid establishment of a gradient in cell density (Figure 1b). Furthermore, we examined the influence of nanotopographic gradients on generating cell gradients. We prepared three groups of nanotopographic gradients, that is, large gradient (Grad. 1, $\theta=0°$), intermediate gradient (Grad. 2, $\theta=15°$), and small gradient (Grad. 3, $\theta=30°$) (Figure 1c, and Figure S2 in the Supporting Information). With the decrease in the nanotopographic gradients from Grad. 1 to Grad. 2 to Grad. 3, the cell gradients decreased accordingly (Figure 1d). In particular, for Grad. 3, the generated cell density was hardly evident. These results demonstrate that controllable cell gradients can be rapidly generated on a nanodendritic silica gradient without any chemical modification.

To investigate the influence of chemical gradients on nanotopographic gradients in generating cell gradients, we performed cell adhesion experiments in parallel on a nanodendritic gradient substrate, on a flat glass surface with a chemical gradient of *n*-octadecyltrichlorosilane/poly(ethylene glycol)silane (OTS/PEG), on substrates with overlapping nanotopographical and chemical gradients in both parallel and antiparallel directions, and on a nanodendritic gradient substrate with OTS (or PEG) modification (Figure 2, and Figure S6, Sections 2–5 and 9 in the Supporting Information). We selected OTS and PEG to construct the chemical gradient by varying surface densities, because they represent the typical chemical cues for promoting and resisting protein absorption, and will promote and repel cellular adhesion, respectively.[6c,21] After incubation for 30 min, a cell gradient was generated on the nanotopographic gradient substrate (Figure 2a,g). In comparison, only a few cells adhered on the glass surface with a chemical gradient of OTS/PEG (Figure 2b,h), suggesting that the chemical gradient cannot induce a cell gradient within such a short period. When the chemical gradient overlapped with the nanotopographic gradient in the parallel direction, a cell gradient was rapidly generated (Figure 2c,i). By contrast, on the substrate with overlapping gradients in the antiparallel direction, there were only a few adhered cells (Figure 2d,j), implying that the chemical gradient offsets the cell gradient induced by the nanotopography, despite its incapability for rapidly generating cell gradients. Moreover, only a few cells unexpectedly adhered on the nanotopographic gradient with OTS modification, probably because the trapped air on the nanodendritic surface hinders the contact of cells with the surface (Figure 2e,k, see details in Figure S6 and Section 9 in the Supporting Information).[22] On the nanotopographic silica gradient with PEG modification, only a few cells were adhered (Figure 2f,l).[21a] These results indicate that a chemical gradient can affect the generation of cell gradients induced by a nanotopographic gradient.

To further understand the mechanism of the nanotopographic gradient for generating a cell gradient, we charac-

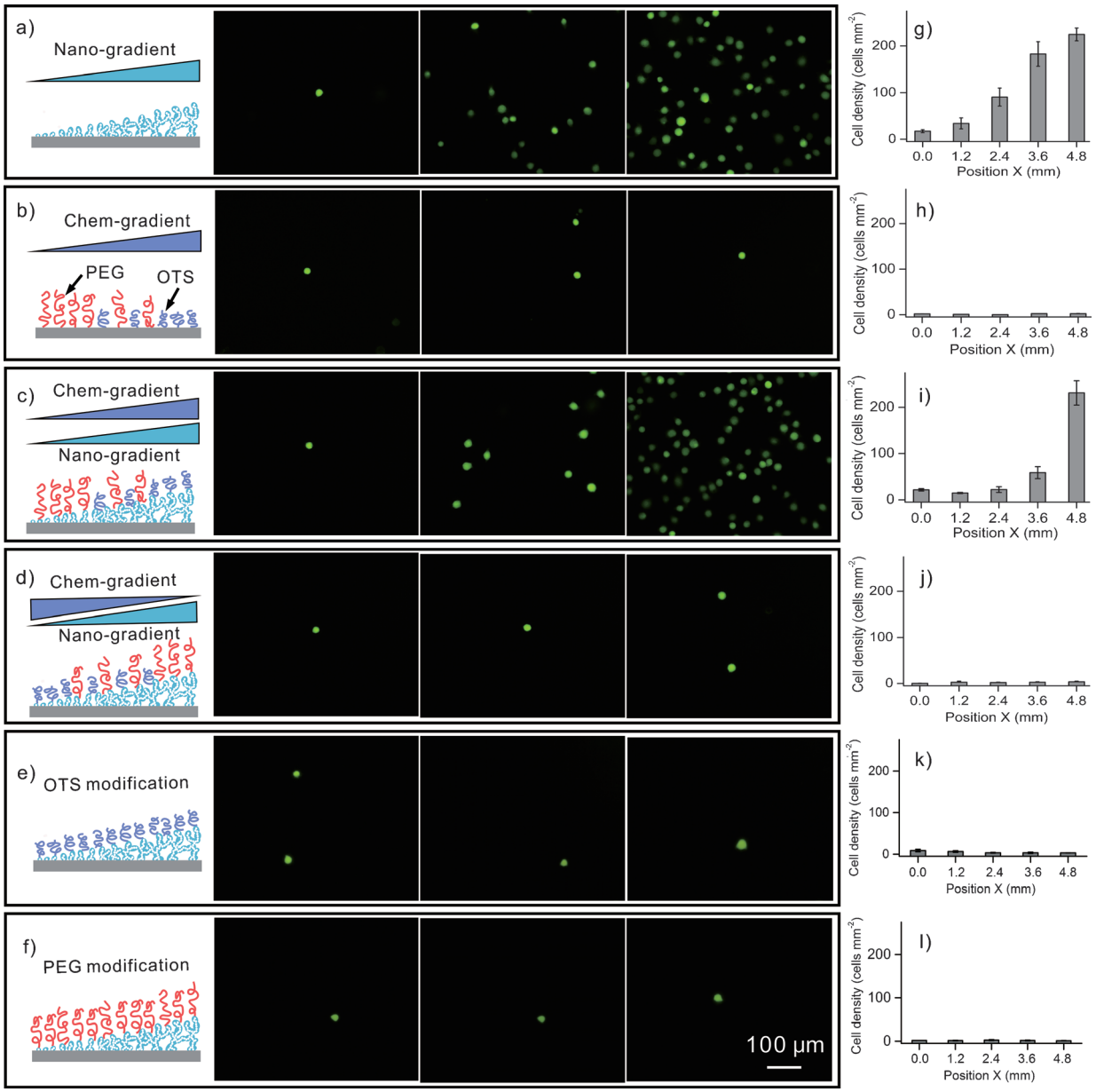

Figure 2. The influence of chemical gradients on cell gradients induced by a nanotopographic gradient. On the nanodendritic gradient substrate (e.g. Grad. 2), a cell gradient was observed (a, g). In comparison, only a few scattered cells and no apparent cell gradient was observed on the glass surface with chemical gradient of OTS/PEG (b, h); see text for details. A cell gradient was generated when the nanotopographic and chemical gradients overlapped in a parallel direction (c, i). By contrast, when they overlapped in an antiparallel direction, only a few cells adhered on the substrate (d, j). Moreover, only a few cells were unexpectedly adhered on the nanotopographic gradient substrate with the OTS modification (e, k); see text for details.[22] On the nanodendritic gradient substrate with modification of PEG, there were only a few cells (f, l). Magnifications are the same for all the fluorescence images. Error bars represent the standard error of mean from three measurements.

terized the morphologies, actin cytoskeleton, and focal adhesion of NIH/3T3 cells on the nanodendritic silica substrate and the flat glass surface (Figure 3, and Figure S3 in the Supporting Information). Extensive filopodia with lengths of about 1.8 to 4.7 μm protruded from cells on the nanodendritic silica substrate, while only a few filopodia were observed for cells on the flat glass surface, indicating enhanced topographic interactions between the nanodendritic structures and nanoscaled filopodia on the cell surface.[15–18] Moreover, the actin cytoskeleton (red) and focal adhesion (green) of NIH/3T3 cells were visualized. Cells on the nanodendritic silica substrate displayed extended actin skeletons and large areas of focal adhesion, while cells on the flat glass surface exhibited nearly spherical actin skeletons and small areas of focal adhesion. This difference further verified the enhanced topographic interactions between the nanodendritic structures and nanoscaled filopodia of the cells[23] and indicated that they contribute to the improved cell adhesion, leading to the rapid generation of cell gradients.

In summary, we have demonstrated a unique approach to rapidly generate cell gradients on bio-inert glass surfaces, by solely introducing a nanodendritic gradient without any

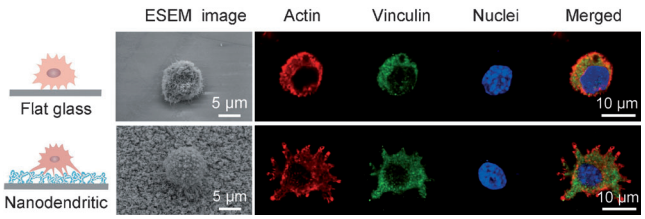

Figure 3. SEM images and immunofluorescence images of NIH/3T3 cells on the bare flat glass surface (top panel) and the bare nanodendritic silica substrate (bottom panel). Immunofluorescent images including actin (red, for actin skeleton), vinculin (green, for focal adhesion), and nuclei (blue). Cells adhered on the nanodendritic silica substrate exhibit more filopodia, more extended actin skeletons, and a larger area of focal adhesion than those on the flat glass substrate. This difference suggests enhanced topographic interactions between the nanodendritic structure and the nanoscaled filopodia of the cells. ESEM images were obtained with a tilt angle of 60°. Magnifications are the same as those in the immunofluorescent images. ESEM images were obtained with a tilt angle of 60°. The scale bars in ESEM images are 5 μm. The immunofluorescent images have the same magnification. Scale bars are 10 μm.

chemical modification. This approach is unique in two aspects: 1) It can induce the rapid generation of controllable cell gradients within only half an hour of cell incubation; 2) the substrate does not require any chemical modification to improve cell adhesion for generating cell gradients. Moreover, this approach is not cell-specific, but can be applied to other cell types, such as MG63 osteoblasts and HeLa cell lines (Figure S7, Supporting Information). The nanodendritic silica gradient can also be easily introduced onto other surfaces, such as titania and alumina substrates, leading to the establishment of cell gradients on such surfaces (Figure S8, Supporting Information). Therefore, we envision that this strategy should find promising applications in the design of functional nano/bio interfaces with controllable cell gradients, such as gradient implants.[5]

Received: November 17, 2013
Published online: February 12, 2014

Keywords: cell gradients · chemical modification · nanotopographic gradient · topographic interaction

[1] J. B. Gurdon, P. Y. Bourillot, *Nature* **2001**, *413*, 797.
[2] S. Thomopoulos, G. R. Williams, J. A. Gimbel, M. Favata, L. J. Soslowsky, *J. Orthop. Res.* **2003**, *21*, 413.
[3] a) E. T. Roussos, J. S. Condeelis, A. Patsialou, *Nat. Rev. Cancer* **2011**, *11*, 573; b) T. M. Keenan, A. Folch, *Lab Chip* **2008**, *8*, 34; c) J. Wu, Z. Mao, H. Tan, L. Han, T. Ren, C. Gao, *Interface Focus.* **2012**, *2*, 337.
[4] a) M. M. Stevens, J. H. George, *Science* **2005**, *310*, 1135; b) W. Song, D. D. Veiga, C. A. Custódio, J. F. Mano, *Adv. Mater.* **2009**, *21*, 1830; c) J. F. Mano, *Biomimetic Approaches for Biomaterials Development*, Wiely-VCH, Weinheim, **2012**.
[5] a) L. Le Guéhennec, A. Soueidan, P. Layrolle, Y. Amouriq, *Dent. Mater.* **2007**, *23*, 844; b) E. Saiz, E. A. Zimmermann, J. S. Lee, U. G. K. Wegst, A. P. Tomsia, *Dent. Mater.* **2013**, *29*, 103.
[6] a) R. R. Bhat, B. N. Chaney, J. Rowley, A. Liebmann-Vinson, J. A. Genzer, *Adv. Mater.* **2005**, *17*, 2802; b) J. K. He, Y. A. Du, J. L. Villa-Uribe, C. M. Hwang, D. C. Li, A. Khademhosseini, *Adv. Funct. Mater.* **2010**, *20*, 131; c) Y. Cai, Y. H. Yun, B.-m. Zhang Newby, *Colloids Surf. B* **2010**, *75*, 115; d) J. A. Genzer, *Annu. Rev. Mater. Res.* **2012**, *42*, 435; e) S. Morgenthaler, C. Zink, N. D. Spencer, *Soft Matter* **2008**, *4*, 419.
[7] N. Zaari, P. Rajagopalan, S. K. Kim, A. J. Engler, J. Y. Wong, *Adv. Mater.* **2004**, *16*, 2133.
[8] A. M. D. Wan, D. J. Brooks, A. Gumus, C. Fischbach, G. G. Malliaras, *Chem. Commun.* **2009**, 5278.
[9] W. Liu, Y. Zhang, S. Thomopoulos, Y. Xia, *Angew. Chem.* **2013**, *125*, 447; *Angew. Chem. Int. Ed.* **2013**, *52*, 429.
[10] a) C. Rappaport, J. P. Poole, H. P. Rappaport, *Exp. Cell Res.* **1960**, *20*, 465; b) A. S. G. Curtis, *J. Cell Biol.* **1964**, *20*, 199.
[11] a) J. S. Miller, K. R. Stevens, M. T. Yang, B. M. Baker, D.-H. T. Nguyen, D. M. Cohen, E. Toro, A. A. Chen, P. A. Galie, X. Yu, R. Chaturvedi, S. N. Bhatia, C. S. Chen, *Nat. Mater.* **2012**, *11*, 768; b) K. Zhang, Y. Ma, LF. Francis, *J. Biomed. Mater. Res.* **2002**, *61*, 551.
[12] A. Yamamoto, S. Mishima, N. Maruyama, M. Sumita, *J. Biomed. Mater. Res.* **2000**, *50*, 114.
[13] H.-W. Kim, J.-H. Song, H.-E. Kim, *J. Biomed. Mater. Res. Part A* **2006**, *79A*, 698.
[14] a) A. S. G. Curtis, M. J. Varde, *Natl. Cancer. Res. Inst.* **1964**, 33, 15; b) K. A. Simon, E. A. Burton, Y. Han, J. Li, A. Huang, Y.-Y. Luk, *J. Am. Chem. Soc.* **2007**, *129*, 4892; c) C. J. Bettinger, R. Langer, J. T. Borenstein, *Angew. Chem.* **2009**, *121*, 5512; *Angew. Chem. Int. Ed.* **2009**, *48*, 5406; d) V. L. S. LaPointe, A. T. Fernandes, N. C. Bell, F. Stellacci, M. M. Stevens, *Adv. Healthc. Mater.* **2013**, DOI: 10.1002/adhm.201200382; e) K. Riehemann, S. W. Schneider, T. A. Luger, B. Godin, M. Ferrari, H. Fuchs, *Angew. Chem.* **2009**, *121*, 886; *Angew. Chem. Int. Ed.* **2009**, *48*, 872; f) B. M. Baker, C. S. Chen, *J. Cell Sci.* **2012**, *125*, 3015; g) M. A. Bucaro, Y. Vasquez, B. D. Hatton, J. Aizenberg, *ACS Nano* **2012**, *6*, 6222.
[15] a) S. Wang, H. Wang, J. Jiao, K.-J. Chen, G. E. Owens, K.-i. Kamei, J. Sun, D. J. Sherman, C. P. Behrenbruch, H. Wu, H.-R. Tseng, *Angew. Chem.* **2009**, *121*, 9132; *Angew. Chem. Int. Ed.* **2009**, *48*, 8970; b) L. Chen, X. Liu, B. Su, J. Li, L. Jiang, D. Han, S. Wang, *Adv. Mater.* **2011**, *23*, 4376; c) H. Liu, Y. Li, K. Sun, J. Fan, P. Zhang, J. Meng, S. Wang, L. Jiang, *J. Am. Chem. Soc.* **2013**, *135*, 7603.
[16] J. Sekine, S.-C. Luo, S. Wang, B. Zhu, H.-R. Tseng, H.-h. Yu, *Adv. Mater.* **2011**, *23*, 4788.
[17] P. Zhang, L. Chen, T. Xu, H. Liu, X. Liu, J. Meng, G. Yang, L. Jiang, S. Wang, *Adv. Mater.* **2013**, *25*, 3566.
[18] G. Yang, H. Liu, X. Liu, P. Zhang, C. Huang, T. Xu, L. Jiang, S. Wang, *Adv. Healthc. Mater.* **2013**, DOI: 10.1002/adhm.201300233.
[19] X. Deng, L. Mammen, H.-J. Butt, D. Vollmer, *Science* **2012**, *335*, 67.
[20] H. Míguez, N. Tétreault, B. Hatton, S. M. Yang, D. Perovic, G. A. Ozin, *Chem. Commun.* **2002**, 2736.
[21] a) K. L. Prime, G. M. Whitesides, *J. Am. Chem. Soc.* **1993**, *115*, 10714; b) T. Satomi, Y. Nagasaki, H. Kobayashi, H. Otsuka, K. Kataoka, *Langmuir* **2007**, *23*, 6698; c) G. B. Sigal, M. Mrksich, G. M. Whitesides, *J. Am. Chem. Soc.* **1998**, *120*, 3464; d) E. Ostuni, B. A. Grzybowski, M. Mrksich, C. S. Roberts, G. M. Whitesides, *Langmuir* **2003**, *19*, 1861.
[22] F. L. Geyer, E. Ueda, U. Liebel, N. Grau, P. A. Levkin, *Angew. Chem.* **2011**, *123*, 8575; *Angew. Chem. Int. Ed.* **2011**, *50*, 8424.
[23] W. Chen, S. Weng, F. Zhang, S. Allen, X. Li, L. Bao, R. H. W. Lam, J. A. Macoska, S. D. Merajver, J. Fu, *ACS Nano* **2013**, *7*, 566.

